Vietnam Journal of Catalysis and Adsorption
Tạp chí xúc tác và hấp phụ Việt Nam

http://jca.edu.vn

Adsorption and dersorption of lead using synthetic hydroxyapatite material

Le Thi Phuong Thao[1,2,3], Ha Manh Hung[1,3], Nguyen Viet Hung[1,3], Vo Thi Hanh[1,2,3], Vu Kim Thu[1], Cong Tien Dung[1,3], Nguyen Tran Tho[4], Le Thi Duyen[1,2,3,*]

[1] *Department of Chemistry, Faculty of Basic Science, Hanoi University of Mining and Geology, 18 Pho Vien, Duc Thang, Bac Tu Liem district, Hanoi, Vietnam*
[2] *HiTech-CEAE Research Team, Hanoi University of Mining and Geology*
[3] *BSASD research group, Faculty of Basic sciences, Hanoi University of Mining and Geology*
[4] *Student, HUS High School for Gifted Students, Hanoi, Vietnam*
**Email: lethiduyen@humg.edu.vn*

ARTICLE INFO

Received: 04/07/2024
Accepted: 18/09/2024
Published: 30/09/2024

Keywords:
Hydroxyapatite; adsorption; desorption; recovery; Pb^{2+} ion

ABSTRACT

The adsorption of Pb^{2+} ions in solution by synthetic hydroxyapatite material was researched. The effects of adsorption time, adsorbent mass, solution pH, and Pb^{2+} ion concentration on adsorption properties were investigated. The Pb^{2+} adsorption efficiency of material can reach 98.7%. Two adsorption isotherm models, Freunlich and Langmuir, were used to evaluate adsorption isotherms. The pseudo-first-order and pseudo-second-order adsorption kinetic models were used to assess the adsorption process's kinetics. Using the electrolysis approach, Pb^{2+} ions were successfully desorbed from the adsorbed HAp material, and were recovered in the form of Pb metal on the cathode surface. Pb recovery efficiency can be as high as 93.84%.

1. Introduction

Technology is developing at a quick pace, which is causing environmental contamination, of which water pollution has become an urgent issue. Nutrients, pesticides, dyes, medications, and heavy metals pollute water and the aquatic environment, endangering human health [1]. The four primary heavy metals that have a substantial impact on human health are lead (Pb), mercury (Hg), cadmium (Cd), and inorganic arsenic. Water pollution induced by these toxic heavy metal ions is not only harmful to the ecosystem due to its high toxicity, but it is also non-biodegradable [2]. Pb is one of the most interesting heavy metals because of its widespread use and extended half-life. Lead-acid batteries, the electroplating sector, electrical technology, steel, and explosives production enterprises are the main sources of lead discharge [3]. Through water consumption, toxic Pb(II) can build up in the body and pose a threat to human health by resulting in birth abnormalities, cognitive impairment, and kidney dysfunction. Learning impairments and intellectual disability are potential consequences of lead exposure, particularly in young [4].

Current methods for removing lead from water include ion exchange [5], membrane filtration, solvent extraction, electrochemical precipitation [6], chemical precipitation [7], and adsorption [8]. Among the methods listed above, the use of solid substances for adsorption is the most effective at separating inorganic pollutants from wastewater. The adsorption method has number advantages over other techniques, including cost-effectiveness in terms of both initial investment and ongoing operation, ease of implementation, and the ability to use a wide range of natural solid adsorbents, simple design, exceptional

https://doi.org/10.62239/jca.2024.057

efficiency in removing harmful contaminants even at low concentration levels, and good material regeneration [3]. Many various types of adsorbents have been and are being investigated, such as kaolin [9], oxide [10], metal-organic frameworks (MOFs) [11], biomaterials [12],... However, eliminating lead from water still presents numerous technological and cost-related challenges. As a result, adsorption research is vital and continues to be of interest in order to improve the quality of existing adsorbents or develop novel adsorbents in order to reduce costs, improve removal efficiency, and, most importantly, material regeneration [3].

Chemical approaches, such as acid solutions (HCl, HNO_3) [12, 13], salt solutions (EDTA or Na_2EDTA [14], $NaNO_3$ [15], and Na_2S [16]) are primarily used in the desorption of lead from adsorbent materials. Pb(II) can be utilized to create cement and composites based on unsaturated polyester resin (UPR) and can also be transformed to Pb(II) phthalate after being desorbed from the cotton adsorbent by 0.5 M HCl solution [17].

Electrochemical approaches for concurrently desorbing metal ions and recovering metals are highly effective and practicable, but just a few studies have been published [18-20]. Our study team also employed electrolysis to desorb Pb^{2+} from the haloysite adsorbent and recover Pb with up to 93.67% efficiency [21].

Calcium hydroxyapatite, often known as hydroxyapatite (HAp), has the formula of $Ca_{10}(PO_4)_6(OH)_2$. In addition to its use in the biomedical field, HAp is a safe, non-toxic adsorbent that is also highly effective at adsorbing metal ions (Cu^{2+}, Pb^{2+}, Cr^{3+}, Co^{2+},...) inorganic anions, organic substances (drugs and dyes), and others [22].

The Pb^{2+} adsorption capacity in water of artificial hydroxyapatite materials, the ability of Pb(II) desorption, and Pb recovery using the electrochemical precipitation method are evaluated in this research.

2. Experimental

Synthesis of HAp powder materials

Using $Ca(NO_3)_2.4H_2O$, $(NH_4)_2HPO_4$, and NH_3 as starting ingredients, HAp powder was made in a water environment by the chemical precipitation process according to Eq. 1 [18]:

$$10Ca(NO_3)_2 + 6(NH_4)_2HPO_4 + 8NH_3 + 2H_2O \rightarrow Ca_{10}(PO_4)_6(OH)_2 + 20NH_4NO_3 \quad (1)$$

The obtained synthetic HAp powder is white and rod-shaped with a specific surface area of 91.42 m^2/g calculated using the Brunauer, Emmett, and Teller (BET) technique.

Investigating the Pb^{2+} adsorption capacity of synthetic HAp powder

The Pb^{2+} adsorption capacity of HAp was tested by introducing a predetermined amount of HAp material to a vessel containing 50 mL of Pb^{2+} solution under the experimental conditions. Contact time, pH, adsorbent mass, and the initial concentration of Pb^{2+} solution were all examined as adsorption process parameters. The adsorption time ranged from 5 to 80 minutes. The pH of the solution was from 2.5 to 6.0. The weight of HAp powder was 0.003 – 0.02 g, and the concentration of the solution ranged from 20 to 140 mg/L. The mixture was then agitated using a magnetic stirrer at 800 rpm. After adsorption and filtration for separating solid particles, the filtered solution was analyzed to quantify residual Pb^{2+} ions using an inductively coupled Plasma mass spectrometry (ICP-MS Thermo Scientific, Germany - ICAP Q ICP-MS, at Hanoi University of Mining and Geology).

The adsorption capacity and efficiency were determined by equations (2) and (3):

$$Q = (C_o - C).V/m \quad (2)$$

$$H = (C_o - C).100/C_o \quad (3)$$

In which: Q (mg/g) and H (%) are the adsorption capacity and adsorption efficiency, respectively; C_o (mg/L) and C (mg/L) are the initial and remaining Pb^{2+} ion concentrations after adsorption, respectively; V (L) is the volume of adsorption solution; m (g) is the mass of HAp.

Desorption of Pb^{2+} ions out of HAp adsorbent and recovery of metallic Pb by electrochemical precipitation method

The cyclic voltammetric curves (CVs) of Pb^{2+} and Pb^{2+}-adsorbed HAp (Pb-HAp) in HCl electrolyte

In the cyclic voltammetry scan experiments, a three-electrode system connected to an Autolab PGSTAT20 potentiostat from Metrohm was used. The working electrode (WE) was a gold electrode (S = 0.0201 cm^2); the reference electrode (RE) was the Ag,AgCl|Cl electrode; and the auxiliary/counter electrode (CE) was the Pt mesh electrode. The CV curve of Pb^{2+}/HCl was achieved using an electrolyte solution of 0.01 M HCl and 0.001 M $Pb(NO_3)_2$. The CV curve of Pb-HAp/HCl was obtained with an electrolytic mixture of 1.0 g of Pb-HAp dispersed in 10 mL of 0.01 M HCl solution. The potential scanning rate was 0.05 V/s with a step of 0.005 V. The scan potential was 0.0 V ~ -0.7 V.

https://doi.org/10.62239/jca.2024.057

Desorption of Pb^{2+} and precipitation of metallic Pb onto the Au electrode

The process of desorption of Pb^{2+} ions from Pb-HAp and precipitation of Pb metal was carried out in an electrolysis cell with three electrodes in constant current mode: WE was a gold plate (geometric area = 1 cm^2), RE was a silver/silver chloride electrode Ag,AgCl|Cl^-, and CE was a large area platinum mesh. The electrolysis process was performed by weighing a determined mass of Pb-HAp powder (obtained when adsorbing Pb^{2+} by HAp under optimal conditions) into 10 mL of 0.01 M HCl solution at room temperature (25°C). In order to ensure that the Pb-HAp powder is evenly distributed throughout the mixture, swirl the mixture with a magnetic stirrer at a speed of 400 rpm for 30 minutes before to electrolysis. The electrolysis processes were set at voltages ≤ - 0.5 V.

The following electrolysis process parameters were examined: current intensity (1 - 7.5 mA/cm^2); mass of adsorbent material (0.1 - 0.3 g); electrolysis time (2 - 10 hours). After electrolysis, the Pb-HAp powder was filtered, cleaned, and dried. The amount of Pb remaining in the powder was determined using the ICP-MS method. The Pb recovery efficiency was determined according to expression:

$$H_{dersorp} = (C_{o,Pb\text{-}HAp} - C_{e,Pb\text{-}HAp}).100/C_{o,Pb\text{-}HAp} \quad (4)$$

In which: $H_{dersorp}$ (%) is the Pb recovery efficiency; $C_{o,Pb\text{-}HAp}$ (ppm) is the Pb^{2+} concentration in the initial Pb-HAp powder; $C_{e,Pb\text{-}HAp}$ (ppm) is the remaining Pb^{2+} concentration in Pb-HAp powder after electrolysis.

3. Results and discussion

The Pb^{2+} adsorption ability of synthetic HAp powder

The adsorption ability of Pb^{2+} on synthetic HAp powder was studied under the following conditions: the mass of HAp changed from 0.003 to 0.02 g/50 mL Pb^{2+} solution of 50 mg/L, pH = 5.3, adsorption time of 60 minutes at room temperature (25°C). The results in Figure 1 show that the synthesized HAp material has good Pb^{2+} adsorption ability. When the HAp mass increased from 0.003 to 0.01 g, the adsorption efficiency increased from 39.1% to 99.7%, while the adsorption capacity decreased from 342.9 mg/g to 234.6 mg/g. When the mass of HAp increased from 0.01 to 0.02 g, the adsorption efficiency was stable while the adsorption capacity gradually decreased. Therefore, to achieve simultaneously high adsorption capacity and adsorption efficiency, a HAp powder mass of 0.01 g was chosen to study Pb^{2+} treatment.

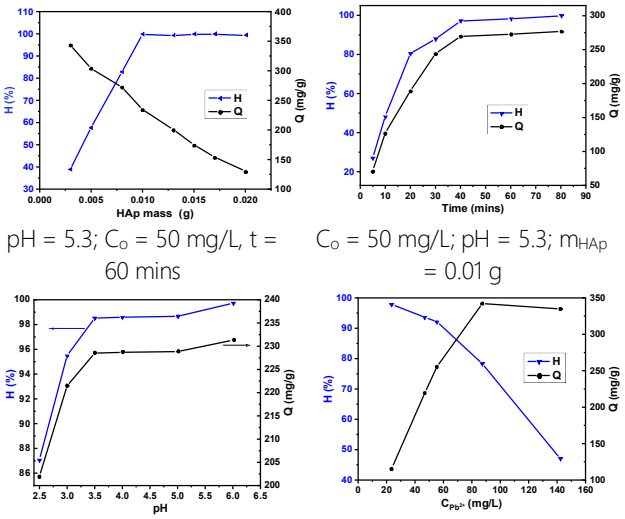

pH = 5.3; C_o = 50 mg/L, t = 60 mins

C_o = 50 mg/L; pH = 5.3; m_{HAp} = 0.01 g

m_{HAp} = 0.01 g; C_o = 50 mg/L; t = 40 mins

m_{HAp} = 0.01 g; pH = 5.3; t = 40 mins

Fig 1: Effect of some factors on the Pb^{2+} adsorption ability of synthetic HAp powder

Figure 1 also shows the results investigating the effect of contact time, solution pH, and initial Pb^{2+} concentration. According to the survey results, the process of adsorption demonstrated the highest adsorption capacity of 228.8 mg/g and adsorption efficiency of 98.7% under the following conditions: adsorption time of 40 minutes, 0.01 g HAp/50 mL of Pb^{2+} solution with concentration of 50 mg/L, and pH = 5.3 (initial pH) at 25°C.

Adsorption isotherm

The isotherm of Pb^{2+} adsorption was evaluated through Langmuir and Freundlich models [23]:

- The Langmuir model equation:

$$\frac{C_e}{Q} = \frac{C_e}{Q_m} + \frac{1}{K_L.Q_m} \quad (5)$$

- The Freundlich model equation:

$$LnQ = LnK_F + \frac{1}{n}.LnC_e \quad (6)$$

where C_e (mg/L) is the equilibrium concentration of Pb^{2+}, Q (mg/g) is the amount adsorbed at equilibrium, Q_m (mg/g) is the maximum adsorption capacity, K_L is the Langmuir coefficient related to the adsorption energy, K_F and n are the constants of the Freundlich model.

The results in Fig. 2 and Table 1 demonstrate that, the Langmuir model (R^2 = 0.99953) is more suitable fit for the experimental data of Pb^{2+} adsorption by HAp than the Freundlich model (R^2 = 0.85221) in research conditions. This aligns with numerous prior studies on HAp adsorbents and the use of HAp in the adsorption of heavy metals [22,24,25]. According to Langmuir, the

https://doi.org/10.62239/jca.2024.057

maximum Pb^{2+} adsorption capacity (Q_{max}) is 340.136 mg/g (Table 1), which is significantly greater than the Pb^{2+} adsorption of HAp-based material [8], or the Pb^{2+} adsorption of some other materials, such as haloysite [21].

Adsorption kinetic

The adsorption kinetics is described by the pseudo-first-order and pseudo-second-order kinetic models using Eqs. 7 and 8, respectively [12].

$$\ln(Q_e - Q_t) = \ln Q_e - k_1.t \quad (7)$$

$$t/Q_t = t/Q_e + 1/(k_2.Q^2_e) \quad (8)$$

where Q_e (mg/g) is the adsorption capacity at equilibrium, Q_t (mg/g) is the adsorption capacity at time t, and k_1 (min^{-1}) and k_2 (g/mg.min) are the pseudo-first-order and pseudo-second-order rate constants, respectively. The results are shown in Fig. 2 and Table 1.

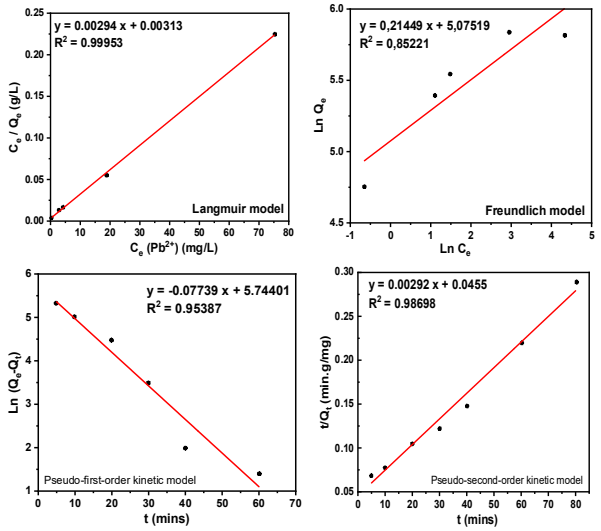

Fig. 2: Adsorption isotherm, kinetic plots of the adsorption of Pb^{2+} onto HAp

According to the results in Table 1, the reliability coefficient R^2 of the pseudo-second-order kinetic model (R^2 = 0.98698) is greater than that of the pseudo-first-order kinetic model (R^2 = 0.95387) and near to unity. Furthermore, the equilibrium adsorption capacity value calculated by the pseudo-second-order kinetic equation ($Q_{e,cal}$) is closer to the maximum adsorption capacity value calculated by the Langmuir equation than the adsorption capacity value calculated by the pseudo-first-order kinetic equation. From there, it is reasonable to argue that the pseudo-second-order kinetic model better describes the Pb^{2+} adsorption process than the pseudo-first-order model. This finding is consistent with prior studies on the adsorption of HAp to heavy metal ions [22,24,25]. The determined adsorption rate constant has a value of $1.874.10^{-4}$ g/mg.min.

Table 1: Experimental parameters calculated according to the Langmuir, Freundlich equations and pseudo-first-order and pseudo-second-order kinetic models

Adsorption isotherm model	Parameter	Value
Langmuir	Q_m (mg/g)	340.136
	K_L	0.939
	R^2	0.99953
Freundlich	K_F	160.00
	n	4.662
	R^2	0.85221
Adsorption kinetic model	**Parameter**	**Value**
Pseudo-first-order	k_1 (min^{-1})	0.07739
	$Q_{e,cal}$ (mg/g)	312.314
	$Q_{e,exp}$ (mg/g)	269.5
	R^2	0.95387
Pseudo-second-order	k_2 (g/mg.min)	$1.874.10^{-4}$
	$Q_{e,cal}$ (mg/g)	342.466
	$Q_{e,exp}$ (mg/g)	269.5
	R^2	0.98698

Adsorption mechanism

The XRD pattern of HAp after Pb^{2+} adsorption (Fig. 3) shows peaks that are characterized as Pb-HAp in addition to HAp. This matches with the proposed mechanism as follows: the adsorption Pb^{2+} on HAp and the exchange Pb^{2+} ions with Ca^{2+} ions in HAp:

$$Ca_{10}(PO_4)_6(OH)_2 + xPb^{2+} \rightarrow Ca_{10-x}Pb_x(PO_4)_6(OH)_2 + xCa^{2+} \quad (7)$$

Furthermore, at low pH, a part of the HAp dissolves in an aqueous solution containing Pb^{2+} ions, therefore the reaction can occur as follows:

$$Ca_{10}(PO_4)_6(OH)_2 + 14H^+ \rightarrow 10Ca^{2+} + 6H_2PO_4^- + 2H_2O \quad (8)$$

$$10Pb^{2+} + 6H_2PO_4^- + 2H_2O \rightarrow Pb_{10}(PO_4)_6(OH)_2 + 14H^+ \quad (9)$$

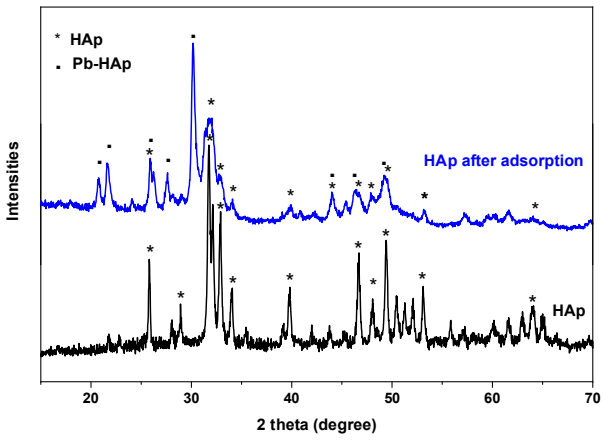

Fig. 3: XRD pattern of the adsorption of Pb^{2+} onto HAp

https://doi.org/10.62239/jca.2024.057

Desorption of Pb^{2+} and recovery of metallic Pb

CV curves of Pb^{2+}/HCl and Pb-HAp/HCl

The results of measuring the CV curves of Pb^{2+}/HCl and Pb-HAp/HCl are shown in Figure 4. The results in Figure 4a shows the appearance of a reduction peak of Pb^{2+} at -0.475 V and an oxidation peak of Pb^{o} at -0.4 V on the CV curve of HCl solution containing 0.001 M $Pb(NO_3)_2$. For the HCl solution containing 1.0 g Pb-HAp, a reduction peak at -0.42 V and an oxidation peak at -0.34 V were observed (Fig. 4b). Thus, both the oxidation peak and the reduction peak in the case of Pb-HAp/HCl have shifted slightly compared to Pb^{2+}/HCl. These peaks are explained due to the following processes occur in solution [26, 27]:

Stage 1: Dissolution of Pb-HAp into Pb^{2+} in HCl environment under the effect of electric current, then the reduction of Pb^{2+} into Pb which precipitates on the electrode surface:

$$Pb^{2+} + 2e \rightarrow Pb$$

Stage 2: Dissolution of Pb into Pb^{2+} (oxidation process):

$$Pb - 2e \rightarrow Pb^{2+}$$

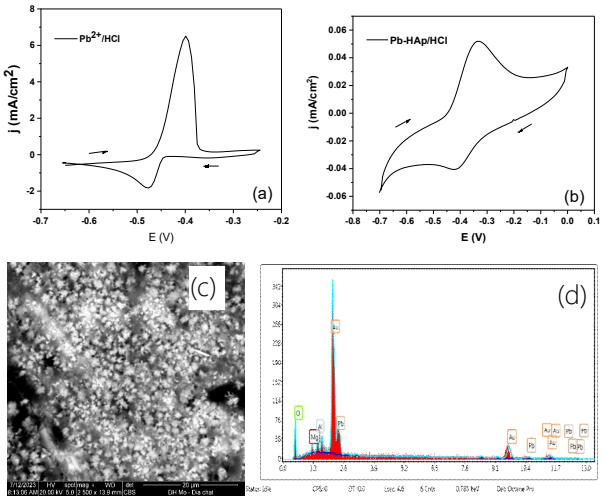

Fig 4: Pb^{2+}/HCl (a) and Pb-HAp/HCl (b) CV curves and SEM-EDX results (c, d) of Au electrode surface after electrolysis of Pb-HAp in HCl

Fig. 4c,d depicts the precipitation of Pb on an Au electrode after Pb-HAp electrolysis. SEM picture reveals that the Au electrode surface after electrolysis has a uniformly adherent metal coating. The EDX spectrum demonstrates that, following electrolysis of Pb-HAp, a Pb peak emerges on the Au surface.

The influence of factors: current density, electrolysis time, mass of Pb-HAp material used on Pb desorption and recovery efficiency was evaluated. The results are shown in Table 2. The results show that, as the current density increases, the reduction rate of Pb^{2+} increases, leading to an increase in the amount of Pb precipitated on the cathode, thus the electrolysis efficiency increases correspondingly. The recovery efficiency Pb also increases as the electrolysis time increases. In case of increasing the mass of Pb-HAp, the recovery efficiency of Pb decreases. This can be explained as follows: when the mass of Pb-HAp powder increases, the amount of Pb^{2+} supplied increases, leading to an increase in the amount of Pb precipitated. However, the amount of Pb precipitate increases less than the increase in Pb-HAp mass, leading to a decrease in recovery efficiency. Reasonable electrolysis conditions to achieve high Pb recovery efficiency (93.84 %) are: j = 5 mA/cm^2; $m_{Pb\text{-}HAp}$ = 0.1 g; t = 8 hours. This recovery efficiency value is much higher than the efficiency of desorption of other heavy metal ions from M-HAp adsorbed materials using chesmitry substances [12].

Table 2: Effect of electrolysis parameters on Pb^{2+} desorption and Pb recovery efficiency

j, mA/cm^2	H_{desorp} %	$m_{Pb\text{-}HAp}$, g	H_{desorp} %	t, hour	H_{desorp} %
t = 5 h; $m_{Pb\text{-}HAp}$ = 0.3 g		*j = 5 mA/cm^2; t = 5 h*		*j = 5 mA/cm^2; $m_{Pb\text{-}HAp}$ = 0.1 g*	
1	44.18	**0.1**	**87.42**	2	70.25
2	56.47	0.2	83.36	3	79.78
3	64.29	0.3	77.66	4	83.28
5	**77.66**			**5**	87.42
7.5	78.05			**6**	90.42
				8	**93.84**
				10	96,23

4. Conclusion

The research reveals that the synthetic HAp material has good Pb^{2+} adsorption ability. At the adsorption conditions of 40-minute adsorption time, 0.01 g HAp/50 mL of Pb^{2+} solution with concentration of 50 mg/L, pH of 5.3 (initial pH), and temperature of 25°C, the adsorption efficiency reached 98.7%. Adsorption isotherms and adsorption kinetics research indicates that the process is consistent with the Langmuir adsorption isotherm model and pseudo-second-order adsorption kinetics. Using electrolysis method with

https://doi.org/10.62239/jca.2024.057

constant current mode, Pb^{2+} was desorbed out of the adsorbed HAp material and successfully recovered in the form of Pb metal. Under the electrolysis conditions: current density j = 5 mA/cm^2, Pb-HAp mass of 0.1 g/10 mL HCl 0.01 M solution; t = 8 hours, Pb was recovered with an efficiency of 93.84%. However, during the desorption process, HAp was dissolved in HCl, therefore HCl solvent can be used to desorb Pb^{2+} from Pb-adsorbed HAp and recover metallic Pb, but it is not acceptable for reuse material.

References

1. H. Ali, E. Khan, I. Ilahi, Journal of Chemistry 2019 (2019) 1. https://doi.org/10.1155/2019/6730305
2. A. Gupta, V. Sharma, K. Sharma, V. Kumar, S. Choudhary, P. Mankotia, B. Kumar, H. Mishra, A. Moulick, A. Ekielski, P.K. Mishra, Materials 14(16) (2021) 4702. https://doi.org/10.3390/ma14164702
3. A.M. Badran, U. Utra, N.S. Yussof, M.J.K. Bashir, Separations 10 (2023). https://doi.org/10.3390/separations10110565
4. Y. Lei, J. Xie, W. Quan, Q. Chen, A. Wang, Prog. Nat. Sci.: Mater. Int. 34 (2024) 122. https://doi.org/10.1016/j.pnsc.2024.02.005
5. S.D. Deshmukh, K.G. Weideman, C.K. Miskin, K. Kisslinger, and R. Agrawal, ACS Omega 6(33) (2021) 21350–21358. https://doi.org/10.1021/acsomega.1c01589
6. H. Jin, Y. Yu, X. Chen, Process Saf. Environ. Prot. 184 (2024) 1011. https://doi.org/10.1016/j.psep.2024.02.044
7. P. Zhang, S. Ouyang, P. Li, Z. Sun, N. Ding, Y. Huang, J. Clean. Prod. 246 (2020) 118728. https://doi.org/10.1016/j.jclepro.2019.118728
8. A.F. Abdelmegeed, M. Sayed, M. Abbas, S.M. Abdel Moniem, R.S. Farag, A.Z. Sayed, S.M. Naga, Ceram. Int. 50 (2024) 36074. https://doi.org/10.1016/j.ceramint.2024.06.420
9. A. Zhang, J. Liu, Y. Yang, Y. Yu, D. Wu, Chem Eng J 451 (2023) 138762. https://doi.org/10.1016/j.cej.2022.138762
10. D.C. Onu, et al., Environ. Nanotechnol. Monit. Manag. 20 (2023) 100818. https://doi.org/10.1016/j.enmm.2023.100818
11. Z. Ke, Z. Chen, Y. Xiao, F. Tang, S. Zhang, J. Mol. Struct. 1307 (2024) 138005. https://doi.org/10.1016/j.molstruc.2024.138005
12. W. Somyanonthanakun, R. Ahmed, V. Krongtong, S. Thongmee, Chem. Phys. Impact. 6 (2023) 100181. https://doi.org/10.1016/j.chphi.2023.100181
13. N.D. Trung, T.D. Phuong, N. Ping, CTU Journal of Innovation and Sustainable Development 4 (2016) 20-27. https://doi.org/10.22144/ctu.jen.2016.039
14. L. Liu, S. Fan, Z. Wang, J. Hu, Arab. J. Chem. 17 (2024) 105669. https://doi.org/10.1016/j.arabjc.2024.105669
15. L. Cutillas-Barreiro, et al., Ecotoxicol. Environ. Saf. 131 (2016) 118–126. http://dx.doi.org/10.1016/j.ecoenv.2016.05.007
16. J. Zhang, X. Xie, C. Liang, W. Zhu, X. Meng. J. Ind. Eng. Chem. 73 (2019) 233–240. https://doi.org/10.1016/j.molliq.2018.08.104
17. K. Nataša, et al., J. Ind. Eng. Chem. 126 (2023) 520–536. https://doi.org/10.1016/j.jiec.2023.06.041
18. P.T. Nam, D.T.M. Thanh, N.T. Phuong, N.T.T. Trang, C.T. Hong, V.T.K. Anh, T.D. Lam, N.T. Thom, Vietnam Journal of Chemistry 59 (2021) 179. https://doi.org/10.1002/vjch.202000148
19. L.T. Duyen, B.H. Bac, Desalination and Water Treatment 317 (2024). https://doi.org/10.1016/j.dwt.2024.100207
20. Q. Song, Q. Xia, X. Yuan, Z. Xu, Resour. Conserv. Recycl. 190 (2023) 106804. https://doi.org/10.1016/j.resconrec.2022.106804
21. T. Le Thi Phuong, D. Le Thi, Vietnam Journal of Catalysis and Adsorption 13 (2024) 123. https://doi.org/10.62239/jca.2024.022
22. L. Wan, B. Cui, L. Wang, Sustain. Chem. Pharm. 38 (2024) 101447. https://doi.org/10.1016/j.scp.2024.101447
23. J. Wang, X. Guo, Chemosphere 258 (2020) 127279. https://doi.org/10.1016/j.chemosphere.2020.127279
24. Y. Si, J. Hou, H. Yin, A. Wang, J. Nanosci. Nanotechnol. 18 (2018) 3484-3491. https://doi.org/10.1166/jnn.2018.14631
25. T. Wang, W. Cao, K. Dong, H. Li, D. Wang and Y. Xu, Chemosphere 352 (2024) 141367. https://doi.org/10.1016/j.chemosphere.2024.141367
26. R.G. Barrads, K. Belinko, and J. Ambros, Canadian Journal of Chemistry 53 (1975) 389. https://doi.org/10.1139/v75-055
27. A.S. Popović, B. Grgur, J. Mater. Sci.: Mater. Electron. 34, article number 1155, (2023). https://doi.org/10.21203/rs.3.rs-2611870/v1